

TRIAXIAL BEHAVIOR OF LIME STABILIZED CLAYS

Member	Y. Doi	Saga University
Member	B. Buensuceso	Saga University
Member	A. Satoh	Saga University
Member	N. Miura	Saga University

I INTRODUCTION

The bearing capacity and settlement of lime stabilized columns are usually evaluated based on the unconfined compressive strength. The effects of confining pressure, therefore, are not considered in design, although numerous studies (Broms, 1984; Miura et al, 1986) have found that the shear strength of lime stabilized clays increase with increasing confining stress. This paper presents the results of a study on the undrained behavior of lime stabilized Ariake clay under triaxial compression conditions, wherein the pre-shear consolidation stress was varied from 0.65 kgf/cm² to 7.8 kgf/cm². Discussions focus mainly on the effects of confining stress on the stress-strain characteristics, including the pore pressure response of lime stabilized clays.

II EXPERIMENTAL DETAILS

The base clay used was soft Ariake clay taken from Kawasoe District, Saga, with the following properties: $\omega=121\%$; $\omega_L=93\%$; $I_p=56\%$; and $G_s=2.64$. The stabilizing agent used was 10% quicklime. Specimens 5 cm diameter and 10 cm high were prepared according to JSSMFE (1990) and cured for 28 days. Standard consolidated undrained (CU) tests (strain rate 0.1%/min) were carried out on fully-saturated, isotropically consolidated specimens with pre-shear consolidation stress (p_o') equal to 0.65, 1.3, 2.6, 3.9, 5.2 and 7.8 kgf/cm².

III RESULTS AND DISCUSSIONS

The deviator stress-axial strain relationships are shown in Fig. 1. Specimens consolidated under low p_o' ($p_o'=0.65\sim 3.9$ kgf/cm²) exhibit very similar stress-strain curves showing a linear ($q-\epsilon$) relationship almost until failure, with failure stress (q_f) of about 10 kgf/cm². Meanwhile, the ($q-\epsilon$) curves for higher p_o' ($p_o'=5.2$ and 7.8 kgf/cm²) were influenced by the confining stress, such that specimens consolidated to higher stresses failed at higher values of q . Post-peak strain softening behavior is seen for all samples, with a residual strength of approximately 8-9 kgf/cm² at very large strains. A stress-strain curve from an unconfined compression test is also shown in Fig. 1. Interestingly, the unconfined strength is almost the same as the undrained triaxial strength under low p_o' . However, a more brittle post-peak behavior, is seen for the unconfined compression test result. Moreover, a slightly lower modulus is observed for the case of the unconfined compression test.

One advantage of triaxial test over unconfined compression test is the measurement of pore pressure. Figure 2 shows the pore pressure development under varying p_o' . In general, higher pore pressures are developed when p_o' is higher. More significantly, dilatant behavior is observed, with the onset of dilatant behavior occurring at lower strains for samples with lower p_o' . The undrained effective stress paths are shown in Fig. 3. Specimens with $p_o'=0.65\sim 3.9$ kgf/cm² exhibit overconsolidated clay characteristics. Elastic behavior is suggested, as the stress paths rise almost vertically until the failure state. For specimens with high p_o' , however, the stress paths are more rounded due to the higher pore pressure development, and fail at high stresses.

The observation that specimens consolidated to low p_o' have nearly identical stress-strain behavior can be explained as follows. For low levels of p_o' , the process of pre-shear consolidation did not affect the specimens too much, such that the pre-shear void ratios were almost the same ($e_o=3.31\sim 3.35$). Considering the fact that lime stabilized clays follow the critical state concepts of a unique relationship between void ratio, q and p' (see Buensuceso, 1990), it is reasonable to expect the same undrained strength (or failure state) for these specimens since the stress paths traverse the same constant void ratio plane and proceed towards the same point on the critical state line. The pore pressure development, however should be different, i.e. the stress paths for specimens with low p_o' (0.65-2.6 kgf/cm²) proceed to the right in the (q,p') plot and that of the specimen with $p_o'=3.9$ kgf/cm² moves towards the left in order to terminate at the same failure point.

On the other hand, when $p_o'=5.2$ and 7.8 kgf/cm^2 , the influence of confining stress could now be seen, since these specimens have been compressed to lower void ratios ($e_o=3.2$ and 3.0 , respectively). Also, some amount of destructuration may have occurred with the application of relatively higher stresses. Again, in accordance with the critical state concept, the specimens with lower void ratios can be expected to fail at higher stresses, since the stress paths move in different constant void ratio planes from that traversed by the specimens with low p_o' .

IV CONCLUSIONS

The following conclusions regarding the triaxial behavior of lime stabilized clays were reached based on the results just presented.

(1) In general, when the volume changes that occur during consolidation are insignificant, no effects of confining pressure were observed and the specimens have the same failure state.

(2) When the applied pre-shear consolidation pressure is high, the consolidation process cause significant reduction of void ratio, such that the specimens consolidated to higher p_o' exhibit higher strengths.

(3) Post-failure dilatant behavior was observed from the $(u-e)$ relationships.

(4) The triaxial stress-strain behavior of lime stabilized clays could be explained by the critical state concepts.

REFERENCES:

- (1) Broms, B. (1984). "The Lime Column method". Seminar on soil improvement and construction techniques in soft ground. Singapore. pp. 120-133.
- (2) Buensuceso, B.R. (1990). "Engineering behavior of lime treated soft Bangkok clay". D.Eng. Dissertation. Asian Institute of Technology, Bangkok.
- (3) Miura, N., Koga, Y. & Nishida, K. (1986). "Dry jet mixing method for dike foundations in the Ariake clay ground". Bull. Res. Inst. Shallow Sea and Tidal Land. Saga Univ. pp. 163-178.

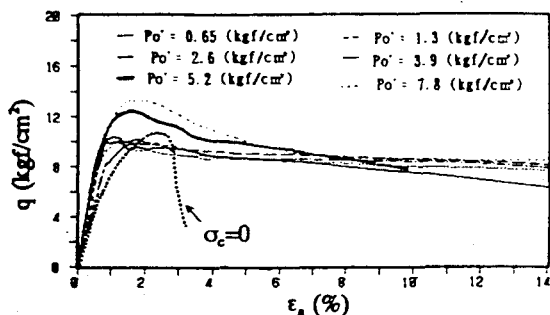


Fig. 1 Stress-strain relationships

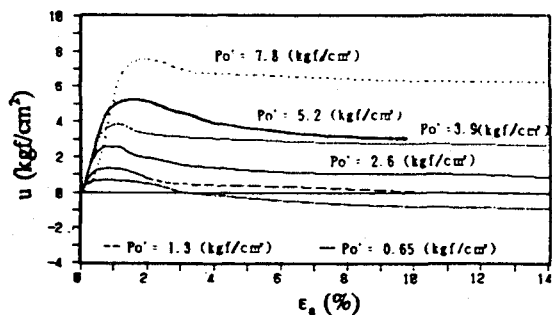


Fig. 2 Pore pressure development

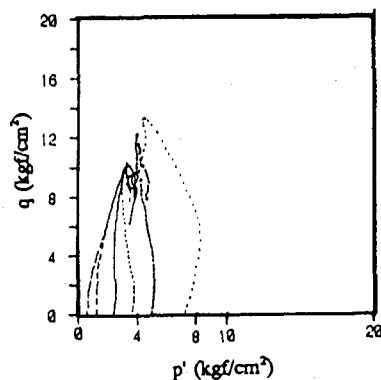


Fig. 3 Effective stress paths